THE JOURNAL OF BIOLOGICAL CHEMISTRY VOL. 285, NO. 11, pp. 8130–8137, March 12, 2010

Effects of Introducing a Single Charged Residue into the Phenylalanine Clamp of Multimeric Anthrax Protective Antigen*

Received for publication, December 10, 2009, and in revised form, January 7, 2010 Published, JBC Papers in Press, January 8, 2010, DOI 10.1074/jbc.M109.093195

Blythe E. Janowiak[1], **Audrey Fischer**[1], **and R. John Collier**[2]

From the Department of Microbiology and Molecular Genetics, Harvard Medical School, Boston, Massachusetts 02115

Multimeric pores formed in the endosomal membrane by the Protective Antigen moiety of anthrax toxin translocate the enzymatic moieties of the toxin to the cytosolic compartment of mammalian cells. There is evidence that the side chains of the Phe^{427} residues come into close proximity with one another in the lumen of the pore and form a structure, termed the Phe clamp, that catalyzes the translocation process. In this report we describe the effects of replacing Phe^{427} in a single subunit of the predominantly heptameric pore with a basic or an acidic amino acid. Incorporating any charged residue at this position inhibited cytotoxicity ≥1,000-fold in our standard assay and caused strong inhibition of translocation in a planar phospholipid bilayer system. His and Glu were the most strongly inhibitory residues, ablating both cytotoxicity and translocation. Basic residues at position 427 prevented the Phe clamp from interacting with a translocation substrate to form a seal against the passage of ions and accelerated dissociation of the substrate from the pore. Acidic residues, in contrast, allowed the seal to form and the substrate to remain firmly bound, but blocked its passage, perhaps via electrostatic interactions with the positively charged N-terminal segment. Our findings are discussed in relation to the role of the Phe clamp in a Brownian ratchet model of translocation.

How the enzymatic moieties of intracellularly acting bacterial toxins cross membranes is not well understood and is a topic of interest in protein structure and function, as well as in bacterial pathogenesis. Anthrax toxin consists of three nontoxic proteins that co-assemble to produce a series of free or cell-bound toxic complexes (1). Two of the proteins, Lethal Factor (LF)[3] and Edema Factor (EF), are enzymes that modify cytosolic targets (2, 3). The third, Protective Antigen (PA), is a receptor-binding and pore-forming protein that transports LF and EF to the cytosol (4). Initially, PA is activated by cellular proteases of the furin family, or by serum proteases (5–8), which cleave the 83-kDa protein into N-terminal 20-kDa and C-terminal 63-kDa fragments. The larger fragment self-associates to form ring-shaped heptamers (prepores), which bind up to three molecules of LF and/or EF, and a smaller population of octamers, which bind up to four molecules of these moieties (9, 10). The resulting hetero-oligomeric complexes then undergo receptor-mediated endocytosis (11–13). Once within the acidic environment of the endosome, the PA moiety is conformationally altered to generate a membrane-inserted pore (14, 15), and LF and EF unfold (16, 17) and translocate across the membrane to the cytosol (18).

Recent electrophysiological studies of anthrax toxin in planar lipid bilayers have shown that the PA pores play an active role in translocating LF and EF across the endosomal membrane. The pore is a mushroom-shaped structure, with a globular cap and a 100-Å long stem with a transmembrane segment at its distal end (Fig. 1). The enzymic moieties bind to the cap via their homologous N-terminal domains (LF_N and EF_N). An unstructured segment containing a high density of both basic and acidic residues is present at the extreme N terminus of LF_N and EF_N, and there is good evidence that this segment initiates N- to C-terminal translocation (17, 19, 20). The blockage of ion conductance through the pore when LF_N, EF_N, or their parent proteins bind is also dependent on this highly charged segment. Translocation of bound ligands through PA pores in planar bilayers may be effected by applying either a pH gradient or a *cis*-positive potential (*e.g.* ~50 mV) and is manifested by the relief of channel blockage (21, 22). The pH gradient emulates the gradient across the endosomal membrane and may provide the major driving force for translocation *in vivo* (21).

A specific phenylalanine residue (Phe^{427}) within the lumen of the cap of the pore, near the junction of the cap with the stem, plays a key role in the PA transport function (Fig. 1) (23). Mutation of Phe^{427} to almost any residue except Trp, Tyr, or Leu causes a loss of the ability of PA to mediate toxicity, and indeed, many Phe^{427} mutations are dominantly negative, in that mixing a low ratio of mutant to wild-type PA together results largely in the formation of nonfunctional oligomers. Mutation of Phe^{427} to Ser, Thr, or His inhibits the translocation function of PA without significantly affecting the conformational transition of the prepore to the pore, whereas some other mutations at this site affect pore formation (24). Inhibition of ion conductance in

* This work was supported, in whole or in part, by National Institutes of Health Grants 1F32 AI077280 (to B. E. J.) and 5R01 AI022021 (to R. J. C.). This work was also supported by New England Regional Center of Excellence Grant A1057159. RJC holds equity in PharmAthene, Inc.

[1] Both authors contributed equally to this work.

[2] To whom correspondence should be addressed: Dept. of Microbiology and Molecular Genetics, Harvard Medical School, 200 Longwood Ave., Boston, MA 02115. Tel.: 617-432-1930; Fax: 617-432-0115; E-mail: jcollier@hms.harvard.edu.

[3] The abbreviations used are: LF, lethal factor; LF_N, N-terminal domain (residues 1–263) of LF; EF, edema factor; EF_N, N-terminal domain of EF; PA, protective antigen; E_{rev}, applied membrane potential at which current is null; DTA, diphtheria toxin catalytic domain; WT, wild-type; MES, 2-(*N*-morpholino)ethanesulfonic acid; $\Delta\psi$, membrane potential; P_o, probability to reside in the open state; $t_{1/2}$, half time of completion of translocation; γ, single-channel conductance.

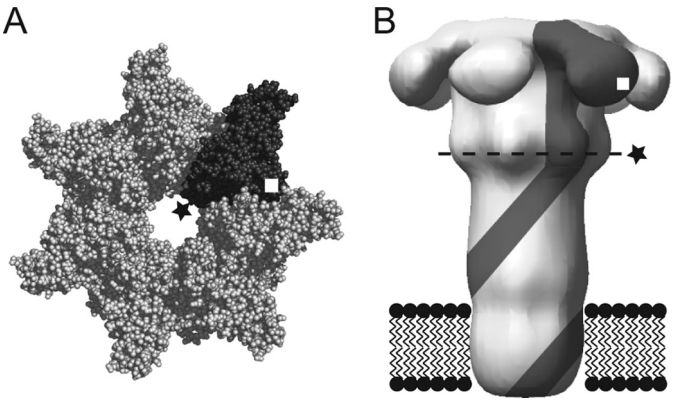

FIGURE 1. **Schematic of heteroheptameric PA mutants.** Prepore (*A*) and membrane-inserted (*B*) PA with a single subunit (*gray*) containing F427*X* (★) and K563C (□) are shown. *Dashed line* in *B* represents predicted location of the Phe clamp. Crystal structure of heptameric PA prepore is from PDB 1TZN (38); membrane-inserted PA is from the reconstruction of negatively stained EM particles (39).

planar bilayers by a translocatable ligand (*e.g.* LF_N) also depends on Phe^{427} (23, 25). Binding of LF_N to wild-type pore results in an almost complete blockage of current, but binding to F427A pores, for example, causes only partial blockage (23, 25).

Electron paramagnetic resonance studies with PA containing a thiol-reactive EPR probe linked to Cys introduced at position 427 suggested that the side chains at this position converge during prepore-to-pore conversion and are brought into in close proximity (≤10 Å) within the lumen of the pore (23). Single-channel conductance values of various Phe^{427} mutants are consistent with the notion that this residue lies at a constriction point in the translocation pathway; the term Phe clamp (or Φ clamp) has been coined for this structure (23). Single-channel traces recorded in the presence of LF_N suggest that the Phe clamp interacts directly with the N-terminal region of the bound ligand to form a seal against the passage of ions.

In an earlier report, we described a protocol for preparing heteroheptamers with an inhibitory mutation in only a single subunit (25). Both F427A and F425A were known to have dominant negative inhibitory effects on toxicity in PA homo-oligomers (26–30), and isolating heteroheptamers with the inhibitory mutation in only one subunit enabled us to characterize the effects of these mutations in greater detail. In the current study we applied the same protocol to isolate a series of heteroheptamers in which Phe^{427} had been replaced with a charged residue in a single subunit. The observed effects of F427D, F427E, F427K, F427R, and F427H on cytotoxicity, translocation, and other activities of the pore offer insights into the structure and function of the Phe clamp.

EXPERIMENTAL PROCEDURES

Materials—Biochemical reagents were purchased from Sigma unless indicated otherwise. Oligonucleotides for mutagenesis were from Integrated DNA Technologies (Coralville, IA). N^{α}-(3-maleimidylpropionyl)biocytin was from Invitrogen, and UltraLink immobilized monomeric avidin was obtained from Pierce. LF_N, LF_N-DTA (20, 27, 31), and $[WT]_6[F427A]_1$ (25) were prepared as described. [^{3}H[rsq]Leucine was from PerkinElmer Life Sciences. *Escherichia coli* BL21 (DE3) used for expression of proteins was grown in ECPM1 medium (32).

Expression and Purification of Proteins—Recombinant WT PA and PA mutants were overexpressed in the periplasm of *E. coli* BL21 (DE3) and purified by anion-exchange chromatography (14). The mutated PA proteins contained two mutations, K563C and F427*X* (where *X* = a charged natural amino acid) (Fig. 1). The proteins were biotinylated using a 10-fold molar excess of N^{α}-(3-maleimidylpropionyl)biocytin at 4 °C overnight and purified over avidin resin (25).

Formation and Purification of Homoheptameric and Heteroheptameric PA_{63} Prepore—WT PA prepore ($[WT]_7$) and homoheptameric PA F427*X*/K563C prepore ($[F427X]_7$) were formed by limited trypsin digestion followed by anion-exchange chromatography (10). Heteroheptamers containing predominantly one mutant subunit were prepared as described (25). Briefly, we first mixed WT PA with biotinylated PA F427*X*/K563C in a 20:1 molar ratio, nicked the mixture with trypsin, and purified the resulting heptamers by anion-exchange chromatography. The resulting preparation was then passed over monomeric avidin, and bound biotinylated heptamers were eluted with 2 mM d-biotin. The product was desalted to remove free biotin and passed over a second monomeric avidin column to ensure the removal of $[WT]_7$.

Cytotoxicity Assays—Cytotoxicity assays were performed as described (28, 29). PA-dependent translocation of LF_N-DTA was reported by the DTA domain, the enzymatic domain of diphtheria toxin, which inhibits protein synthesis. Translocation of the DTA domain into CHO-K1 cells was determined by measuring the incorporation of [^{3}H]leucine into protein after a 16-h incubation with varying concentrations of PA heptamers and 100 nM LF_N-DTA at 37 °C under 5% CO_2. The data were plotted as averages of at least three experiments ($n \geq 3$), with standard errors shown as bars. EC_{50} values were calculated from the fit of the curves (IGOR Pro Software, version 6.0.3.1; Wavemetrics, Inc., Lake Oswego, OR).

Macroscopic Electrophysiology—Planar phospholipid bilayer experiments were performed in a Warner Instruments Planar Lipid Bilayer Work station (BC 525D, Hamden, CT). Planar bilayers were painted (33) onto a 200-μm aperture of a Delrin cup in a Lucite chamber, with 3% 1,2-diphytanoyl-*sn*-glycerol-3-phosphocholine in *n*-decane (Avanti Polar Lipids, Alabaster, AL). One-ml aliquots of buffer were added to the cup and the chamber, and both compartments were stirred constantly. *Cis* (side to which PA prepore and LF_N were added) and *trans* compartments contained 100 mM KCl, 1 mM EDTA, and 10 mM each sodium oxalate, potassium phosphate, and MES, pH 5.5. Macroscopic current responses to steps in voltage were recorded as described (20); $n \geq 3$. The membrane potential, $\Delta\psi$, is defined as $\Delta\psi = \psi_{cis} - \psi_{trans}$, where $\psi_{trans} \equiv 0$ mV.

Macroscopic PA_{63} Channel Formation, LF_N Conductance Block, and Translocation under the Influence of ΔpH—Once a membrane was formed in the planar lipid bilayer system, PA prepore (25 pM) was added to the *cis* compartment, which was held at a $\psi = +5$ mV with respect to the *trans* compartment. After appropriate current increase, the *cis* compartment was perfused with ~10 ml of non-PA-containing buffer at a flow rate of ~3 ml/min to remove any free PA. Once the current was

constant, LF_N was added to the *cis* compartment (1 μg/ml), and its binding to PA channels was monitored by the decrease in conductance. The *cis* compartment was perfused again after LF_N addition to eliminate free ligand. Initial values of dissociation represent the fraction conductance unblocked by LF_N (n = 3) over time. The rate of dissociation of LF_N over time was calculated based on the slopes of the fitted curves (IGOR Pro Software, version 6.0.3.1). Translocation was initiated by raising the pH of the *trans* compartment to pH 7.2 with 2 M KOH while maintaining the *cis* compartment pH at 5.5. Translocation was quantified by monitoring the half-time to complete alleviation of conductance block ($t_{1/2}$). Experiments for each PA protein tested were normalized to control experiments where KOH was added to the *trans* compartment in the absence of LF_N to adjust for current changes due to salt addition alone. The kinetics of translocation were monitored at $\psi = +5$ mV by the rise in current; $n \geq 3$.

Single-channel Electrophysiology—Single-channel measurements were obtained under conditions similar to macroscopic current recordings, but with a 100-μm aperture membrane. The 1-ml *cis* and *trans* compartments contained 1 M KCl and 10 mM MES at pH 5.5, and current was measured over a range of applied membrane potentials. Increments of ~0.1 ng of PA_{63} heteroheptamer prepore were added until a single channel was observed. For PA blocking experiments with LF_N, the *cis* and *trans* compartments contained 100 mM KCl, 1 mM EDTA, and 10 mM each sodium oxalate, potassium phosphate, and MES, pH 5.5. After channel formation LF_N was added to the *cis* compartment (final concentration, 1 μg/ml). Data were analyzed using Clampfit version 10.0 software (Axon Instruments, Sunnyvale, CA) and Microsoft Excel. Analysis was performed on 10-s records. Single-channel conductance was calculated from Gaussian fits to current amplitude histograms; $n \geq 3$. Percent block of PA channel activity by LF_N was determined as $1 - P_o$ (the probability of the channel to reside in the open state).

Ion-selectivity Measurements—Anion/cation selectivity of the PA channel was measured by determining the dependence on the activity ratio of KCl in the *cis versus trans* compartments of the membrane potential at which the current across the membrane equals zero (E_{rev}). Channel activity for each of the proteins tested was elicited under symmetric conditions of 0.1 M KCl, 10 mM MES, pH 5.5, followed by serial additions of 19 μl of 3.6 M KCl to the *cis* compartment. The E_{rev} was measured for symmetric *cis*/*trans* solutions and after each addition. E_{rev} was plotted against the activity ratio (activity of KCl in *cis*/activity of KCl in *trans*) and fit to the Goldman-Hodgkin-Katz equation to determine the probability to conduct K^+ (p_K)/probability to conduct Cl^- (p_{Cl}); $n \geq 3$. Activity coefficients were obtained from Appendix 8.10, Table 2 in Robinson and Stokes (34); the KCl concentration was assumed to be equal to the K^+ concentration as well as the Cl^- concentration.

RESULTS

Effects of Single-subunit Phe^{427} Mutations on Cytotoxicity—We prepared five hetero-oligomeric forms of the prepore, each containing a positively or negatively charged residue at position 427 of a single subunit. The protocol yields predominantly heptamers and was used earlier to generate $[WT]_6[F427A]_1$ and $[WT]_6[F425A]_1$ (25). EC_{50} values were determined in our standard cytotoxicity assay, in which LF_N-DTA, the catalytic moiety of diphtheria toxin (DTA) fused to LF_N, is delivered to the cytosol, inhibiting protein synthesis and causing cell death. EC_{50} values of heteroheptamers containing either a basic or an acidic residue in the Phe clamp were found to be at least 3 orders of magnitude higher than that of the $[WT]_7$ (Fig. 2 and Table 1). The most active forms, $[WT]_6[F427D]_1$ and $[WT]_6[F427R]_1$, were ~1,000-fold less active than $[WT]_7$, and the least active, $[WT]_6[F427E]_1$ and $[WT]_6[F427H]_1$, showed no activity at the highest concentrations tested (1 μM). In con-

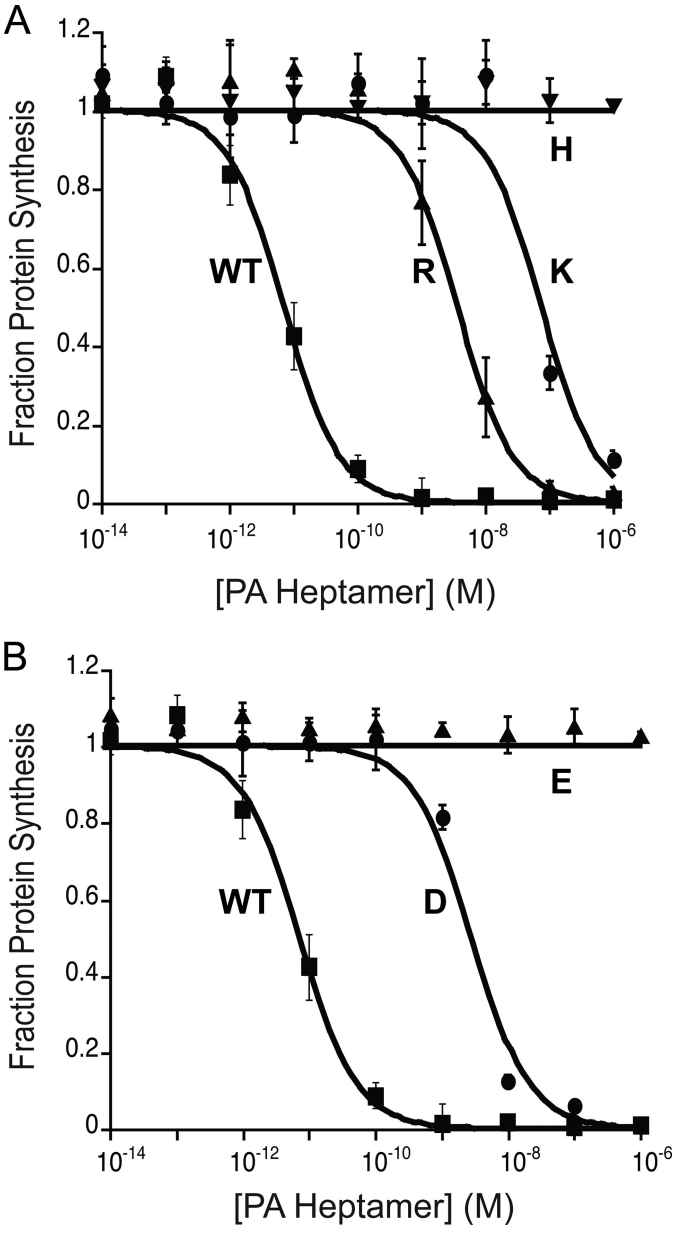

FIGURE 2. **Effect on cytotoxicity of adding a single charged residue into the Phe clamp.** Cells were incubated with PA heptamers at the indicated concentrations in the presence of 100 nM LF_N-DTA. After 16 h, we measured the incorporation of [^{3}H]leucine into protein over a 1-h period. *A*, $[WT]_6[F427K]_1$ (●), $[WT]_6[F427R]_1$ (▲), $[WT]_6[F427H]_1$ (▼), and $[WT]_7$ (■). *B*, $[WT]_6[F427D]_1$ (●), $[WT]_6[F427E]_1$ (▲), and $[WT]_7$ (■).

TABLE 1

Comparison of properties of heteroheptamer mutants as determined by cytotoxicity experiments and electrophysiology of macroscopic and single channels of PA formed in planar lipid bilayers

Heptamer	EC_{50}[a]	LF_N block single[b]	LF_N block macro[c]	LF_N dissociation[d]	LF_N translocation $t_{1/2}$[e]	(+) γ[f]	(−) γ[g]	p_K/p_{Cl}[h]
	nM	*%*	*%*	*%/min*	*s*	*pS*	*pS*	
$[WT]_7$	0.026 ± 0.007	97 ± 2	98 ± 1	0.2 ± 0.1	22.9 ± 0.3	154 ± 2	154 ± 3	39
$[WT]_6[F427D]_1$	29 ± 6	91 ± 4	99 ± 1	0.4 ± 0.1	960 ± 10	425 ± 8	344 ± 7	44
$[WT]_6[F427E]_1$	>1000	97 ± 3	99 ± 1	0.3 ± 0.1	>10,000	531 ± 7	387 ± 12	22
$[WT]_6[F427R]_1$	37 ± 9	63 ± 2	74 ± 2	6.2 ± 0.3	326 ± 5	122 ± 7	224 ± 8	1.5
$[WT]_6[F427K]_1$	770 ± 30	61 ± 3	65 ± 2	5.5 ± 0.4	619 ± 11	123 ± 7	274 ± 11	2
$[WT]_6[F427H]_1$	>1000	62 ± 2	69 ± 3	4.8 ± 0.2	>10,000	124 ± 5	173 ± 5	6
$[WT]_6[F427A]_1$	2.2 ± 0.3[i]	67 ± 2	91 ± 4[i]	7.2 ± 0.5[i]	292 ± 7[i]	310 ± 17	320 ± 12	10

[a] EC_{50} values representing the cytotoxicity of the protein when combined with LF_N-DTA on CHO-K1 cells were calculated from the curves shown in Fig. 2.
[b] Percentage of total conductance blocked upon adding LF_N to a single PA channel formed on planar lipid bilayers at $\Delta\psi = +5$ mV. LF_N block was assayed over a range of applied membrane potentials for each mutant and then calculated for $\Delta\psi = +5$ mV as the limits of signal detection often precluded direct measurement at $\Delta\psi = +5$ mV.
[c] Percentage of total conductance blocked upon adding LF_N to macroscopic PA channels formed on planar lipid bilayers.
[d] Percentage of total conductance blocked lost over time upon perfusion of excess LF_N associated with macroscopic PA channels formed on planar lipid bilayers.
[e] Translocation rate expressed in time required for half of bound LF_N to pass through PA, as calculated by determining the slope of the tangent of the curves shown in Fig. 3*C*.
[f] Average single-channel conductance over a range of applied positive membrane potentials (Fig. 4*A*). pS, picosiemens.
[g] Average single-channel conductance over a range of applied negative membrane potentials. pS, picosienems.
[h] Probability to conduct K^+/probability to conduct Cl^- as calculated from the curves shown in Fig. 4*B*.
[i] The values shown for EC_{50}, $t_{1/2}$, and LF_N block and dissociation for $[WT]_6[F427A]_1$ were calculated based on data reported previously (25).

trast, incorporating either a single Asn or Gln residue into the Phe clamp caused relatively little inhibition of cytotoxicity (5-fold and 8-fold, respectively; data not shown).

Effects of LF_N on Ion Conductance through Hetero-oligomeric Pores—Binding of LF or LF_N, to pores formed from $[WT]_7$ prepore causes rapid and virtually complete (~98%) blockage of ion conductance, as measured macroscopically in planar phospholipid bilayers (20, 22). With pores containing a single Glu or Asp in the Phe clamp, the blockage by saturating levels of LF_N was at least as rapid and complete as that observed with $[WT]_7$ pores. In contrast, pores containing a Lys, Arg, or His residue showed greatly reduced blockage (reduction ~30%) (Table 1 and Fig. 3*A*). Results consistent with these findings were observed in single-channel ion-conductance recordings in the presence and absence of LF_N (Table 1 and Fig. 3*B*). Channels with an acidic residue in the Phe clamp gave a blocking pattern by LF_N (final concentration 1 μg/ml) similar to that seen with $[WT]_7$ channels, with fast transitions to and from the open state and prolonged periods in the closed state, reflecting prolonged occlusion times by the cargo protein (35). With a basic residue, however, no transitions to the fully open state were seen, and there were fast, short lived transitions between closed and intermediate states.

Effects of Single-subunit Mutations on Dissociation of LF_N—To probe the effects of single-subunit Phe^{427} mutations on the interaction of the pore with LF_N, we first measured the rate of dissociation of pore-bound LF_N into the *cis* compartment. LF_N was bound under symmetric acidic conditions (pH 5.5), and macroscopic current was monitored as the *cis* chamber was perfused with the same buffer. As shown in Fig. 3*A* and Table 1, with pores containing a Glu or an Asp in the Phe clamp, as with WT pores, the current increased at a low rate (<0.5%/min) over a perfusion period of 5 min, and thus the pores remained firmly blocked by LF_N over this period. In contrast, with pores containing a Lys, Arg, or His in the Phe clamp, the current increased ~10-fold faster over the same period, reflecting much more rapid dissociation.

Effects of Single-subunit Mutations on Translocation of LF_N—If, after brief perfusion of the *cis* compartment, we raised the pH of the *trans* compartment to neutrality, bound LF_N was induced to translocate across the membrane. Translocation of LF_N through $[WT]_7$ channels was complete within less than a min ($t_{1/2}$ ~23 s) under these conditions, whereas translocation through the mutant heptameric channels was ~10- to ~440-fold slower (Fig. 3*C* and Table 1). The relative activities of the various heteroheptamers in this assay were similar to their activities in the cytotoxicity assay (Fig. 2). Values of $t_{1/2}$ of translocation ranged from 326 s for $[WT]_6[F427R]_1$, the most active heteroheptamer, to >10,000 s for $[WT]_6[F427E]_1$ and $[WT]_6[F427H]_1$, the least active ones (Table 1).

Effects on Ion Conductance and Selectivity—We characterized the single-channel ion-conductance properties of the heteroheptamers in planar 1,2-diphytanoyl-*sn*-glycerol-3-phosphocholine bilayers. The *cis* and *trans* compartments were filled with 1 M KCl, pH 5.5, and traces were recorded at +50 mV and −50 mV. $[WT]_7$ and $[WT]_6[F427A]_1$ exhibited an ohmic current response, with symmetric single-channel conductance (γ) at positive and negative potentials. In contrast, all of the heteroheptamers showed asymmetric γ values (Table 1). Either Glu or Asp in the Phe clamp caused an increase in γ at both positive and negative membrane potentials. Basic residues, on the other hand, caused a decrease at positive potentials and an increase at negative potentials (Table 1). The $[WT]_7$ channel inactivates under negative membrane potentials, and the acidic residues allowed some of the WT inactivation characteristics to be maintained. However, $[WT]_6[F427R]_1$ and $[WT]_6[F427K]_1$ exhibited significantly reduced inactivation, and the inactivation for $[WT]_6[F427H]_1$ was completely abolished (data not shown). Although the $[WT]_7$ channel is seen to transition to the fully closed state at least once within a 10-s time scale, no transitions to the fully closed state were observed with any of the mutant heteroheptameric channels (Fig. 4*A*).

We measured the ion selectivity of each heteroheptamer to determine the extent to which the cation selectivity of the wild-type PA pore had been altered. Heteroheptamers with an acidic residue in the Phe clamp displayed similar selectivity to $[WT]_7$, but those with a basic residue exhibited significantly reduced selectivity (Fig. 4*B* and Table 1), such that the flux of Cl^- was closer in magnitude to that of K^+.

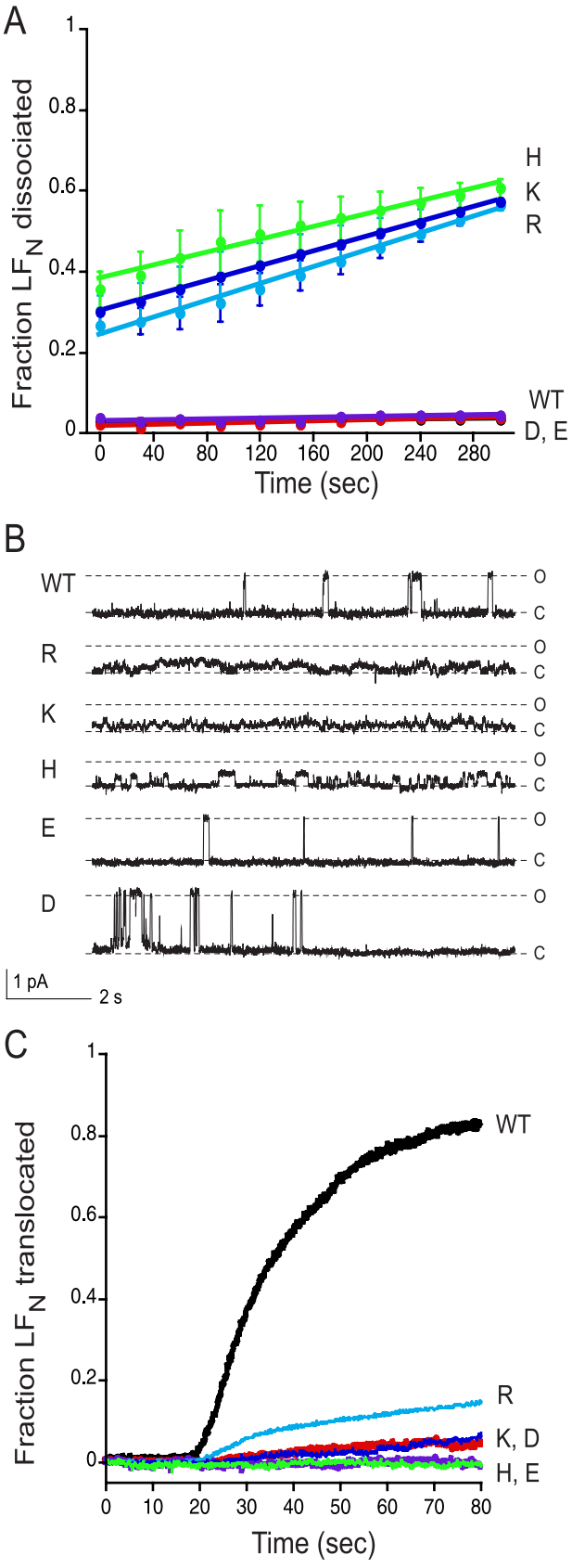

FIGURE 3. **Effect on conductance block of LF_N of adding a single charged residue into the Phe clamp.** *A*, macroscopic conductance was measured at symmetrical pH of 5.5 and $\Delta\psi = +5$ mV for $[WT]_7$ (*black circles*), $[WT]_6[F427K]_1$ (dark *blue circles*), $[WT]_6[F427R]_1$ (*light blue circles*), $[WT]_6[F427H]_1$ (*green circles*), $[WT]_6[F427D]_1$ (*orange circles*), and $[WT]_6[F427E]_1$ (*purple circles*). The channels were blocked with 10 nM LF_N, and then dissociation of LF_N was monitored over time during perfusion of the *cis* compartment. *B*, representative single-channel currents of heteroheptameric PA wild type and mutant channel activity blocked by the addition of 1 μg/ml LF_N to the *cis* compartment, recorded at $\Delta\psi = +20$ mV in 0.11 M KCl. *C* and *O* denote the closed and open states, respectively. *C*, translocation of LF_N through macroscopic PA channels. At time 0, translocation was initiated by adding 2 M KOH to the *trans* compartment to raise the pH to 7.2; there was an ~20-s mixing delay in this system with both compartments continuously stirred. Representative data are shown from $n \geq 3$ trials.

DISCUSSION

There is evidence that translocation through the PA_{63} pore is driven by a transmembrane proton gradient, and we have proposed a Brownian ratchet model of this process that depends on protonation and deprotonation of acidic residues of the translocating polypeptide (21, 23, 24, 36). The pore is known to be strongly cation-selective, reflecting an electrostatic barrier that discriminates against the passage of negatively charged ions. This barrier would also be expected to discriminate against the passage of anionic side chains of Glu or Asp residues of polypeptides in transit through the pore. Because such side chains would spend a greater fraction of time in the protonated, uncharged state when on the acidic, endosomal side of this barrier than on the neutral, cytosolic side, their diffusion across the barrier would occur preferentially in the endosome-to-cytosol direction. Thus, ratcheting of a polypeptide through the pore from the endosome to the cytosol would be predicted, based simply on the proton gradient, the electrostatic barrier within the pore, and Brownian motion. This model has received support from demonstration that an essentially nontitratable anionic group (SO_3^-) introduced at any of a variety of locations within LF_N serves as a stop-translocation signal (36).

Translocation of polypeptides through the pore must involve a delicate balance of interactions between the transporter and the cargo. Clearly, the Phe clamp must accommodate all of the various side chain chemistries of translocatable proteins, but must not bind any particular group too tightly, lest translocation be impeded or arrested. Our working hypothesis is that the phenyl side chains of Phe^{427} directly contact the translocating polypeptide chain and form a pliable surface that conforms to the various side-chain structures of the polypeptide, generating an ion-proof seal that preserves the pH gradient that drives translocation.

The exact location of the electrostatic barrier within the pore is not known, but mutating Phe^{427} to Ala caused the pore to become less selective for K^+ over Cl^- and lowered the barrier to translocation of LF_N bearing an SO_3^- group (36). These findings, together with the fact that two acidic residues, Asp^{425} and Asp^{426}, are immediately adjacent to Phe^{427}, suggest that the main barrier lies at the level of the Phe clamp. Our finding that incorporating an acidic residue into the Phe clamp did not significantly affect the selectivity of the channel for cations, whereas a basic residue reduced the selectivity, is consistent with this hypothesis.

We found that replacement of Phe^{427} with either an acidic or a basic residue in a single subunit of multimeric PA_{63} inhibited cytotoxicity by $\geq 10^3$ in our standard assay (Fig. 2). This remarkable effect of a single charged residue explains the dom-

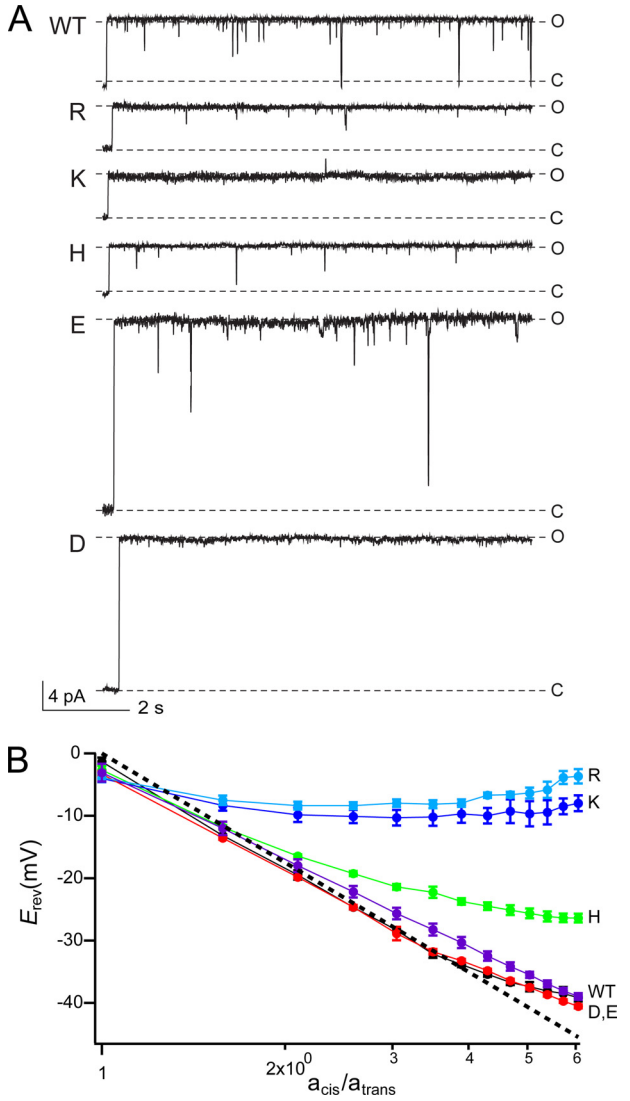

FIGURE 4. **Effects on single-channel conductance and ion selectivity of adding a single charged residue into the Phe clamp.** *A*, representative single-channel currents of PA wild type and heteroheptameric mutants recorded at $\Delta\psi = +50$ mV in 1 M KCl. *C* and *O* denote the closed and open states, respectively. The γ of wild type is symmetric over positive and negative potentials (154 ± 3 picosiemens); however, the heteropheptamer mutations all have asymmetric γ with respect to membrane potential polarity (see Table 1 for details). *B*, ion selectivity of PA_{63} channel is sensitive to single subunit mutation from Phe^{427} to a charged residue. The E_{rev} *versus* the activity ratio of KCl (a_{cis}/a_{trans}) is plotted for $[WT]_7$ (*black circles*), $[WT]_6[F427E]_1$ (*purple circles*), $[WT]_6[F427D]_1$ (*red circles*), $[WT]_6[F427H]_1$ (*green circles*), $[WT]_6[F427K]_1$ (*dark blue circles*), and $[WT]_6[F427R]_1$ (*light blue circles*). Ideal cation selectivity is shown as a *dashed line*. WT PA and mutations of Phe^{427} to acidic residues retain strong cation selectivity, whereas mutations to His, Arg, or Lys have low ion selectivity (see Table 1 for fits to data).

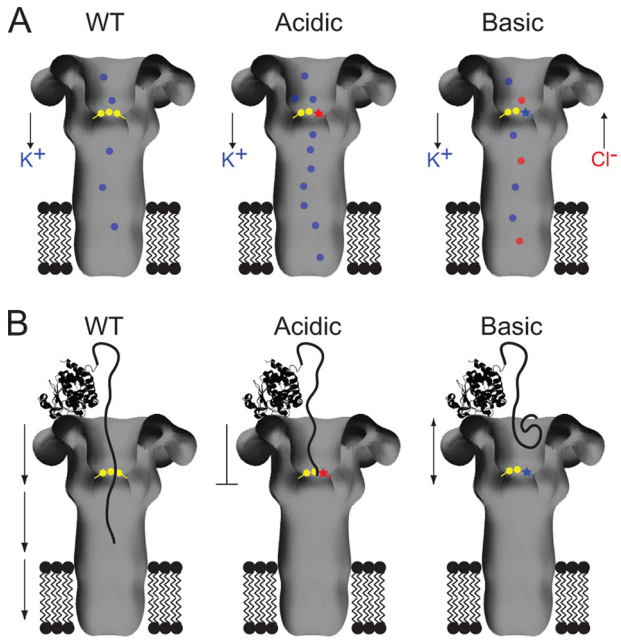

FIGURE 5. **Model of how the charged mutations disrupt native functions of the Phe clamp.** *A*, schematic comparing ion conductance through WT and mutant PA channels is shown. WT PA and acidic mutant channels preferentially conduct K^+ ions, whereas basic mutant PA channels allow the passage of K^+ and Cl^-. Acidic and basic mutants allow an overall increase in ion conductance. The Phe clamp is indicated by *yellow hexagons*, mutations to acidic and basic residues by a *red* and *blue star*, respectively. K^+ ions are indicated as *blue dots* and Cl^- ions as *red dots*. *B*, schematic of productive LF_N translocation through WT PA channels and deficient LF_N translocation through mutant channels containing a single acidic or basic residue in the Phe clamp. The acidic mutation results in a strong persistent block of the PA channel by LF_N, whereas the basic mutation generates a repulsion to the LF_N resulting in an intermediate block state. Conventions hold from *A*; LF_N is shown as a *ribbon structure* of the PDB 1J7N (19) with extended loop entering the PA pore.

inant negative phenotype of these mutations. The importance of charge *per se* in causing the inhibition of pore function is indicated by the small effects on cytotoxicity (<10-fold) of incorporating an Asn or a Gln residue into the Phe clamp. It should be noted that Asn and Gln are structural analogs of His as well as Asp and Glu.

The nature of the effects observed depended on the sign of the charge introduced into the Phe clamp. With the acidic replacements, there was a 3- and 4-fold increase in single-channel conductance for Asp and Glu, respectively, whereas the native cation selectivity was maintained (Fig. 4). We attribute these observations to a significant alteration in constriction diameter based upon the pore size estimation model proposed by Hille (35). Conversely, the presence of a basic residue apparently maintained a similar architecture with altered cation selectivity (Fig. 5*A*). His ablated voltage-dependent inactivation of ion conductance, whereas Lys and Arg allowed at least some sensitivity to applied voltage to be maintained.

An acidic residue did not impair the ability of LF_N to block ion conductance in macroscopic measurements and did not significantly alter the blocking pattern in single-channel measurements. Thus, as in the wild-type pore, the Phe clamp interacted with the polypeptide substrate to form a seal that almost completely blocked ion conductance, transitioning to the open state briefly every couple of seconds (Fig. 3, *A* and *B*); and there was minimal dissociation of the polypeptide during a several-minute perfusion of the *cis* compartment (Fig. 3*A*). In contrast, with a basic residue the ability of LF_N to block ion conductance was significantly reduced (~30%). Furthermore, there were major changes in the pattern of channel opening and closing in single-channel traces (Fig. 3*B*), and significant dissociation of LF_N occurred during perfusion of the *cis* compartment (Fig. 3*A*). Thus, a basic residue prevented the formation of a tight and durable interaction of the Phe clamp with the polypeptide substrate, whereas an acidic residue did not diminish the interaction.

These findings support current thinking about the interaction of the Phe clamp with LF_N. The first ~30 N-terminal residues of LF_N are unstructured and densely populated with acidic and basic residues. This segment is predicted to have a net positive charge under acidic conditions, and there is evidence that the positive charge functions to attract the N-terminal tract into the acidic lumen of the prepore or pore and mediate its interaction with the Phe clamp. Thus, if one deletes this tract, LF_N loses the ability to block ion conductance through the pore, and this ability is restored when one replaces the tract with one containing a His_6 tag (20). Details of the interaction of the tract with the Phe clamp are unknown, but we hypothesize an electrostatic interaction with Asp^{425} and/or Asp^{426}, immediately adjacent to Phe^{427} (37). There may also be a contribution from cation-π interactions between positively charged residues of the tract and phenyl rings of the clamp. This contribution is not determinative, however, because the homoheptameric F427L pore functions reasonably well (23). The blockage of current by LF_N suggests that the N-terminal tract threads at least part way through the Phe clamp even in the absence of a transmembrane proton gradient.

In the context of this model, we can understand how incorporating a basic residue into the Phe clamp might disrupt the clamp interaction with the cationic N-terminal tract of LF_N, either by electrostatically repelling the tract or by interacting with side chains of Asp^{425} and/or Asp^{426} and perturbing the structure of the clamp (Fig. 5*B*). In contrast, incorporating an acidic residue can be envisioned to enhance the electrostatic interaction of the cationic N-terminal tract of LF_N with the clamp. However, increased conductance, resulting from alteration of the native architecture of the pore, may preclude productive translocation (Fig. 5*B*).

Cytotoxicity mediated by the heteroheptamers correlated well with the kinetics of translocation across planar bilayers. All charged residues strongly inhibited translocation, with Glu and His showing the largest effects. We assume, therefore, that the effects on translocation are primarily responsible for the inhibition of cytotoxicity. As suggested by the lowered affinity of the substrate protein for the pore, inhibition of translocation by a basic residue in the Phe clamp may be due in large part to disruption of the interaction of the Phe clamp with the cationic N-terminal tract of LF_N. For those polypeptides that manage to thread part way through the Phe clamp, a basic residue incorporated into the clamp could inhibit the passage of basic residues of the translocating polypeptide by electrostatic repulsion and inhibit the passage of acidic residues by electrostatic attraction. His may promote leakage of protons to a greater degree than Lys or Arg, thereby dissipating the proton gradient more effectively and causing a greater effect on toxicity.

An acidic residue in the Phe clamp may inhibit translocation by concurrently modifying the luminal architecture at or near the constriction point and by tightly binding the basic N-terminal region of LF_N. For polypeptides that thread through the clamp, passage is inhibited by electrostatic repulsion or attraction with acidic and basic residues, respectively. The especially strong effect of Glu over Asp may result from stronger distortion of the Phe clamp constriction. In the final analysis, the effects of replacing a single Phe^{427} residue in the pore with a charged residue are complex and appear to result both from perturbation of the seal against ion (proton) conductance formed by the Phe clamp and from electrostatic interactions of the introduced acidic or basic side chain with charged side chains the translocating polypeptide.

Acknowledgments—We thank Dr. Robin Ross and the Biomolecule Production Core of New England Regional Center of Excellence for helping with the production of proteins used in this study.

REFERENCES

1. Young, J. A., and Collier, R. J. (2007) *Annu. Rev. Biochem.* **76,** 243–265
2. Alfano, R. W., Leppla, S. H., Liu, S., Bugge, T. H., Herlyn, M., Smalley, K. S., Bromberg-White, J. L., Duesbery, N. S., and Frankel, A. E. (2008) *Mol. Cancer Ther.* **7,** 1218–1226
3. Chen, D., Misra, M., Sower, L., Peterson, J. W., Kellogg, G. E., and Schein, C. H. (2008) *Bioorg. Med. Chem.* **16,** 7225–7233
4. Finkelstein, A. (1994) *Toxicology* **87,** 29–41
5. Ezzell, J. W., Jr., and Abshire, T. G. (1992) *J. Gen. Microbiol.* **138,** 543–549
6. Goldman, D. L., Zeng, W., Rivera, J., Nakouzzi, A., and Casadevall, A. (2008) *Clin. Vaccine Immunol.* **15,** 970–973
7. Klimpel, K. R., Molloy, S. S., Thomas, G., and Leppla, S. H. (1992) *Proc. Natl. Acad. Sci. U.S.A.* **89,** 10277–10281
8. Molloy, S. S., Bresnahan, P. A., Leppla, S. H., Klimpel, K. R., and Thomas, G. (1992) *J. Biol. Chem.* **267,** 16396–16402
9. Kintzer, A. F., Thoren, K. L., Sterling, H. J., Dong, K. C., Feld, G. K., Tang, II, Zhang, T. T., Williams, E. R., Berger, J. M., and Krantz, B. A. (2009) *J. Mol. Biol.* **392,** 614–629
10. Wigelsworth, D. J., Krantz, B. A., Christensen, K. A., Lacy, D. B., Juris, S. J., and Collier, R. J. (2004) *J. Biol. Chem.* **279,** 23349–23356
11. Gordon, V. M., Leppla, S. H., and Hewlett, E. L. (1988) *Infect. Immun.* **56,** 1066–1069
12. Singh, Y., Klimpel, K. R., Goel, S., Swain, P. K., and Leppla, S. H. (1999) *Infect. Immun.* **67,** 1853–1859
13. Singh, Y., Leppla, S. H., Bhatnagar, R., and Friedlander, A. M. (1989) *J. Biol. Chem.* **264,** 11099–11102
14. Miller, C. J., Elliott, J. L., and Collier, R. J. (1999) *Biochemistry* **38,** 10432–10441
15. Nassi, S., Collier, R. J., and Finkelstein, A. (2002) *Biochemistry* **41,** 1445–1450
16. Krantz, B. A., Trivedi, A. D., Cunningham, K., Christensen, K. A., and Collier, R. J. (2004) *J. Mol. Biol.* **344,** 739–756
17. Thoren, K. L., Worden, E. J., Yassif, J. M., and Krantz, B. A. (2009) *Proc. Natl. Acad. Sci. U.S.A.* **106,** 21555–21560
18. Wesche, J., Elliott, J. L., Falnes, P. O., Olsnes, S., and Collier, R. J. (1998) *Biochemistry* **37,** 15737–15746
19. Pannifer, A. D., Wong, T. Y., Schwarzenbacher, R., Renatus, M., Petosa, C., Bienkowska, J., Lacy, D. B., Collier, R. J., Park, S., Leppla, S. H., Hanna, P., and Liddington, R. C. (2001) *Nature* **414,** 229–233
20. Zhang, S., Finkelstein, A., and Collier, R. J. (2004) *Proc. Natl. Acad. Sci. U.S.A.* **101,** 16756–16761
21. Krantz, B. A., Finkelstein, A., and Collier, R. J. (2006) *J. Mol. Biol.* **355,** 968–979
22. Zhang, S., Udho, E., Wu, Z., Collier, R. J., and Finkelstein, A. (2004) *Biophys. J.* **87,** 3842–3849
23. Krantz, B. A., Melnyk, R. A., Zhang, S., Juris, S. J., Lacy, D. B., Wu, Z., Finkelstein, A., and Collier, R. J. (2005) *Science* **309,** 777–781
24. Sun, J., Lang, A. E., Aktories, K., and Collier, R. J. (2008) *Proc. Natl. Acad. Sci. U.S.A.* **105,** 4346–4351
25. Janowiak, B. E., Finkelstein, A., and Collier, R. J. (2009) *Protein Sci.* **18,** 348–358
26. Leppla, S. H. (2001) *Nat. Med.* **7,** 659–660
27. Mourez, M., Yan, M., Lacy, D. B., Dillon, L., Bentsen, L., Marpoe, A., Maurin, C., Hotze, E., Wigelsworth, D., Pimental, R. A., Ballard, J. D.,

Collier, R. J., and Tweten, R. K. (2003) *Proc. Natl. Acad. Sci. U.S.A.* **100,** 13803–13808
28. Sellman, B. R., Mourez, M., and Collier, R. J. (2001) *Science* **292,** 695–697
29. Sellman, B. R., Nassi, S., and Collier, R. J. (2001) *J. Biol. Chem.* **276,** 8371–8376
30. Singh, Y., Khanna, H., Chopra, A. P., and Mehra, V. (2001) *J. Biol. Chem.* **276,** 22090–22094
31. Milne, J. C., Blanke, S. R., Hanna, P. C., and Collier, R. J. (1995) *Mol. Microbiol.* **15,** 661–666
32. Bernard, A., and Payton, M. (1995) in *Current Protocols in Protein Science* (Coligan, J. E., Dunn, B. M., Speicher, D. W., Wingfield, P. T., and Ploegh, H. L., eds) pp. 5.3.1–5.3.18, John Wiley and Sons, New York
33. Mueller, P., and Rudin, D. O. (1963) *J. Theor. Biol.* **4,** 268–280
34. Robinson, R. A., and Stokes, R. H. (1965) *Electrolyte Solutions*, 2nd Ed., Butterworths, London
35. Hille, B. (2001) *Ion Channels of Excitable Membranes*, Third Ed., Sinauer Associates, Sunderland, MA
36. Basilio, D., Juris, S. J., Collier, R. J., and Finkelstein, A. (2009) *J. Gen. Physiol.* **133,** 307–314
37. Melnyk, R. A., and Collier, R. J. (2006) *Proc. Natl. Acad. Sci. U.S.A.* **103,** 9802–9807
38. Lacy, D. B., Wigelsworth, D. J., Melnyk, R. A., Harrison, S. C., and Collier, R. J. (2004) *Proc. Natl. Acad. Sci. U.S.A.* **101,** 13147–13151
39. Katayama, H., Janowiak, B. E., Brzozowski, M., Juryck, J., Falke, S., Gogol, E. P., Collier, R. J., and Fisher, M. T. (2008) *Nat. Struct. Mol. Biol.* **15,** 754–760